



Mordenite-incorporated PVA–PSSA membranes as electrolytes for DMFCs

S.D. Bhat^a, A.K. Sahu^a, C. George^b, S. Pitchumani^a, P. Sridhar^a, N. Chandrakumar^b,
K.K. Singh^c, N. Krishna^c, A.K. Shukla^{a,d,*}

^a Central Electrochemical Research Institute, Karaikudi 630 006, India

^b Department of Chemistry, Indian Institute of Technology Madras, Chennai 600 036, India

^c Advanced Technologies Group, Applied Materials Inc., Santa Clara, CA 95052, USA

^d Solid State and Structural Chemistry Unit, Indian Institute of Science, Bangalore 560 012, India

ARTICLE INFO

Article history:

Received 29 December 2008

Received in revised form 2 May 2009

Accepted 9 May 2009

Available online 18 May 2009

Keywords:

DMFC

Methanol permeability

Mordenite composites

NMR imaging

ABSTRACT

Composite membranes with mordenite (MOR) incorporated in poly vinyl alcohol (PVA)–polystyrene sulfonic acid (PSSA) blend tailored with varying degree of sulfonation are reported. Such a membrane comprises a dispersed phase of mordenite and a continuous phase of the polymer that help tuning the flow of methanol and water across it. The membranes on prolonged testing in a direct methanol fuel cell (DMFC) exhibit mitigated methanol cross-over from anode to the cathode. The membranes have been tested for their sorption behaviour, ion-exchange capacity, electrochemical selectivity and mechanical strength as also characterized by Fourier transform infrared spectroscopy and thermogravimetric analysis. Water release kinetics has been measured by magnetic resonance imaging (NMR imaging) and is found to be in agreement with the sorption data. Similarly, methanol release kinetics studied by volume-localized NMR spectroscopy (point resolved spectroscopy, PRESS) clearly demonstrates that the dispersion of mordenite in PVA–PSSA retards the methanol release kinetics considerably. A peak power-density of 74 mW/cm² is achieved for the DMFC using a PVA–PSSA membrane electrolyte with 50% degree of sulfonation and 10 wt.% dispersed mordenite phase. A methanol cross-over current as low as 7.5 mA/cm² with 2 M methanol feed at the DMFC anode is observed while using the optimized composite membrane as electrolyte in the DMFC, which is about 60% and 46% lower than Nafion-117 and PVA–PSSA membranes, respectively, when tested under identical conditions.

© 2009 Elsevier B.V. All rights reserved.

1. Introduction

Direct methanol fuel cells (DMFCs) have reached a high level of development and are now almost universally referred to as the sixth fuel cell type. In terms of applications, they are set to function as power sources for a range of mobile applications. This position has largely been brought about by the convenience of storage of the liquid fuel [1]. At present, DMFCs employ Nafion, a proton-conducting perfluorosulfonic acid polymer membrane as electrolyte that also acts as a physical separator to prevent methanol cross-over from the anode to the cathode. However, methanol cross-over from anode to cathode across the Nafion membrane brings about a mixed potential at the cathode causing loss of fuel and cell polarization. Efforts are therefore being expended to find alternative proton-conducting membranes for DMFCs that could address the aforesaid problems [2–5]. One such effort has been to employ modified-Nafion membranes as also the membranes based

on non-fluorinated and partially fluorinated hydrocarbon-based polymers in the DMFCs [6–16]. Cost-effective natural polymeric membranes like chitosan doped with either phosphotungstic acid (PTA) or poly acrylic acid (PAA) have also been reported as potential methanol barriers without affecting their proton conductivity [17,18]. But these membranes are prone to excessive swelling in aqueous medium that reduces their mechanical strength and limits their use in DMFCs.

Ionomeric membranes based on partially sulfonated polystyrene and its blends with PVA were also reported to exhibit good proton conduction with methanol barrier properties [19,20]. Ironically, however, these authors did not evaluate methanol cross-over characteristic of these membranes in a DMFC. Blend membranes based on sulfonated poly(ether ether ketone) and poly(vinylidene fluoride) have also been evaluated and it is conjectured that sulfonation affects the DMFC performance [21]. Nafion induction in sulfonated poly vinyl alcohol to realize a composite membrane has also been reported and the influence of sulfonation level in the membrane on the performance of a DMFC has been studied [22]. PVA and poly(styrene sulfonic acid-co-maleic anhydride) semi-interpenetrating network have also been studied as proton-conducting membrane that preferentially

* Corresponding author at: Central Electrochemical Research Institute, Karaikudi 630 006, India. Tel.: +91 4565 227777; fax: +91 4565 227779.

E-mail address: shukla@sscu.iisc.ernet.in (A.K. Shukla).

permeates water and restricts methanol cross-over in DMFCs [23–25].

Generally, PVA-based membranes are better methanol barriers than Nafion membranes [26], and follow the principle of pervaporation, wherein sorption of water molecules takes place at the interface of the membrane followed by diffusion across the membrane due to a concentration gradient (rate-determining step) with subsequent desorption into vapor phase. The aforesaid steps are responsible for realizing higher sorption during the operation of a DMFC. Such a situation provides the possibility to custom design membranes to match the above characteristics and the choice for identifying new composite polymeric membranes for DMFCs that offer higher sorption of water with a barrier to methanol.

In the literature [27], it has been demonstrated that PVA–PSSA blend is a potential proton-conducting membrane with lower methanol cross-over in relation to Nafion-117 membrane. In this communication, we have incorporated mordenite (MOR) as a dispersed phase to PVA–PSSA tailored with 50% degree of sulfonation to realize a composite membrane for application in DMFCs. Mordenite is a proton-conducting methanol impermeable zeolite with regular pore sizes providing selective separation of molecules based on their size and shape. Mordenite also helps separating components on the basis of preferential adsorption where the strong adsorption of one component blocks or hinders the phases of the other components. We have designed and carried out NMR imaging and volume-localized NMR spectroscopy studies that help visualize water and methanol permeation, respectively, across PVA–PSSA membranes with varying percentage of dispersed mordenite phase. Our quantitative imaging studies corroborate that water permeation is related to sorption data. Further, methanol permeation across these membranes has been directly measured by volume-localized spectroscopy which confirms that mordenite content reduces methanol permeation. Accordingly, these studies further validate the utility of spatially resolved NMR in designing and evaluating membrane electrolytes for fuel cell applications. Using the PVA membrane with 50% degree of sulfonation of PSSA and 10 wt.% dispersed mordenite, it has been possible to reduce the methanol cross-over current to about 7 mA/cm² with 2 M methanol feed at the DMFC anode, which is about 60% and 46% lower than the methanol cross-over current observed for Nafion and PVA–PSSA membranes, respectively, tested under identical conditions.

2. Experimental

2.1. Materials

Poly vinyl alcohol (average $M_w = 89,000$ – $98,000$ g mol⁻¹; degree of hydrolysis, 99%) and glutaraldehyde (GA) (25 wt.% solution in water) were procured from S.D. Fine Chemicals. Polystyrene sulfonic acid (18 wt.% in water) and polystyrene sulfonic acid (30 wt.% in water) were obtained from Aldrich and Alfa Aesar chemicals, respectively. All chemicals were used as received. Toray TGP-H-120 was procured from E-tek (US). Vulcan XC-72R carbon, Pt/Ru (60 wt.% in 1:1 atomic ratio) and Pt/C (40 wt.% Pt on Vulcan XC-72R carbon) were obtained from Alfa Aesar (Johnson Matthey) Chemicals. Deionised (DI) water (conductivity 18.4 MΩ cm) from a Millipore system was used during the experiments. The sub-micron sized mordenite (MOR) powder with Si/Al = 40 was obtained from National Chemical Laboratory, Pune (India).

2.2. Membrane preparation

PVA–PSSA membranes were prepared by solution casting technique. In brief, 30 mL of 5 wt.% PVA aqueous solution was prepared by dissolving required amount of PVA in water at 333 K followed

by its stirring until a clear solution was obtained. The solution thus obtained was allowed to cool to room temperature (~303 K) and 0.3 mL of GA solution was added to it gradually followed by its stirring for 3–4 h. The resultant solution was cast as a membrane on a flat Plexiglass plate by evaporating the solvent at room temperature. Similarly, PVA–PSSA blend membranes with PSSA of varying degree of sulfonation between 40% and 50% were obtained. PSSA content was kept at 25 wt.% with respect to the PVA in all the blend membranes. PVA–PSSA–MOR membranes with varying amounts of mordenite, namely 3, 5, 10 and 15 wt.%, were also obtained in a similar manner. All the membranes were immersed in 0.5 M aqueous H₂SO₄ solution for 2 h at room temperature (~303 K) for further doping and cross-linking followed by copious washing with DI water to expel any residual H₂SO₄. The thickness of the membranes was ~160 μm.

2.3. Ion-exchange capacity and degree of sulfonation

Ion-exchange capacity (IEC) indicates the number of milliequivalents of ions in 1 g of the polymeric membrane while the degree of sulfonation (DS) refers to the average number of sulfonic groups present in PSSA. To estimate IEC and DS, membranes of similar weights were soaked in 50 mL of 0.01N sodium hydroxide solutions for 12 h at room temperature [28] and 10 mL of this solution was titrated against 0.01N sulfuric acid. The sample was regenerated with 1N hydrochloric acid, washed copiously with water to remove acid and dried to a constant weight and IEC was estimated from Eq. (1) given below.

$$IEC = \frac{(B - P)0.01 \times 5}{m} \quad (1)$$

where IEC = ion-exchange capacity (in mequiv./g), B = amount of sulfuric acid used to neutralize blank sample solution in mL, P = amount of H₂SO₄ used to neutralize the membrane soaked solution in mL, 0.01 = normality of H₂SO₄, 5 = the factor corresponding to the ratio of the amount of NaOH used to soak the membrane to the amount used for titration, and m = polymeric membrane mass in g. The degree of sulfonation was calculated by matching the relationship between DS and IEC akin to the procedure described elsewhere [29] and was found to be ~ 40% and 50%, respectively.

2.4. Sorption measurements

For sorption measurements, circularly cut (diameter = 2.5 cm) membranes were dipped in deionised water for 24 h to attain equilibrium. The samples were surface dried with a tissue paper and initial mass values were recorded on a single-pan digital microbalance (Sartorius, Germany) within an accuracy of ±0.01 mg. The samples were then dried in a hot air oven at 343 K for 12 h and their weights were measured. The % sorption was calculated from Eq. (2) given below.

$$\% \text{ sorption} = \left(\frac{W_\infty - W_0}{W_0} \right) \times 100 \quad (2)$$

where W_∞ and W_0 refer to the weights of sorbed and dry membranes, respectively.

2.5. Proton conductivity

Proton conductivity measurements were performed on PVA, and PVA–PSSA (40% and 50% sulfonation) blend and PVA–PSSA (50% sulfonation)–MOR (3, 5, 10 and 15 wt.%) composite membranes in a two-probe cell by ac impedance technique. The conductivity cell comprised two stainless steel electrodes, each of 20 mm diameters. The membrane sample was sandwiched between the two stainless steel electrodes fixed in a Teflon block and kept in a closed

glass container. The ionic conductivity data for the membranes were obtained under fully humidified condition (100%) by keeping DI water at the bottom of the test container and equilibrating for around 24 h. Subsequently, conductivity measurements were conducted between 303 and 373 K in a glass container with a provision to heat. The temperature was constantly monitored with a thermometer kept inside the container adjacent to the membrane. ac impedance spectra of the membranes were recorded in the frequency range between 1 MHz and 10 Hz with 10 mV amplitude using an Autolab PGSTAT 30. The resistance value associated with the membrane conductivity was determined from the high-frequency intercept of the impedance with the real axis. The membrane conductivity was calculated from the membrane resistance, R , from the Eq. (3) given below.

$$\sigma = \frac{l}{RA} \quad (3)$$

where σ is the proton conductivity of the membrane in S/cm, l is the membrane thickness in centimeters and A is the cross-sectional area of the membrane samples in cm^2 .

2.6. Physicochemical characterization

Universal testing machine (UTM) (Model AGS-J, Shimadzu, China) with an operating head load of 10 kN was used to study the mechanical properties of the membranes. Cross-sectional area of the sample was obtained from the width and thickness of the membrane sample. The test samples were prepared in the form of dumb-bell shaped object as per ASTM D-882 standards. The sample film was then placed in the sample holder of the machine. The film was stretched at a cross-head speed of 1 mm/min and its tensile strength was estimated from Eq. (4) given below.

$$\text{tensile strength (N/mm}^2\text{)} = \frac{\text{maximum load}}{\text{cross-sectional area}} \quad (4)$$

Surface micrographs for PVA–PSSA (50% sulfonation) and PVA–PSSA (50% sulfonation)–MOR (10 wt.%) composite membranes were obtained using JEOL JSM 35CF scanning electron microscope (SEM). Gold film of thickness <100 nm was sputter coated on the membranes, using a JEOL Fine Coat, Ion Sputter–JFC-1100 unit, prior to their study under SEM. Thermogravimetric analysis (TGA) for PVA, PVA–PSSA (40% sulfonation), PVA–PSSA (50% sulfonation), PVA–PSSA (50% sulfonation)–MOR (10 wt.%) and Nafion-117 membranes were conducted, using a SDT Q600 V8.2 TGA/DTA Instrument (US) in the temperature range 298–793 K at a heating rate of 278 K/min, with nitrogen flushed at 200 mL/min. The FTIR spectra for PVA, PVA–PSSA (40% sulfonation), PVA–PSSA (50% sulfonation) and PVA–PSSA (50% sulfonation)–MOR (10 wt.%) membranes were obtained using a Nicolet IR 860 spectrometer (Thermo Nicolet, Nexus-670) in the range 1800–800 cm^{-1} . Average contact angle and surface wetting energy measurements were conducted on these composite membranes using a Surface Electro Optics Model Phoenix-300 unit by Sessile drop method.

2.7. Spatially resolved NMR characterization

Kinetic studies of water release by the membranes (release of water from equilibrated membrane sacs to surrounding D_2O) were carried out on a Bruker Biospec 47/40 system operating at 200 MHz and employing a 112/72 ^1H resonator. The membrane ‘sac’ equilibrated in water was dropped in D_2O and a set of 64×64 multislice gradient echo images were acquired in order to select a suitable slice for the kinetic studies. Gradient echo studies are satisfactory for these measurements of water release from the relatively homogeneous sacs, while permitting rapid image acquisition. A slice passing through the center of the sac was selected in each case from

the set of multislice images and single slice gradient echo imaging was then carried out as a function of time. The first measurement on the selected slice in each case was initiated ca. 9–13 min after dropping the water-equilibrated sac in D_2O . The sac diameter ranged from ~ 5 to 10 mm. The relevant image parameters were: coronal images, 10° pulse flip angle, echo time $\text{TE} = 3.57$ ms, repetition time $\text{TR} = 300$ ms, field of view (FOV) = 3 cm, slice thickness = 1 mm and number of averages $\text{NA} = 8$.

Methanol release studies were also undertaken. It may be noted that owing to the relatively low concentration of methanol in water, selective NMR imaging of methanol is not very practical, except at high fields: recall that the relative chemical shift between H_2O and the methyl group of CH_3OH is ca. 1.5 ppm. Furthermore, the direct imaging of species at low concentration imposes limitations on the time course studies, since sensitivity is effectively reduced in presence of the read gradient required for imaging. On the other hand, volume selective high resolution spectroscopy offers an opportunity to track the process of methanol release, employing outer volume suppression, as well as water suppression in the voxel of interest, which is located outside the sac. In this high resolution scenario, a 1.5 ppm chemical shift difference is now a convenient handle to readily distinguish the species of interest. The permeation of methanol through membrane sacs saturated with 2 M CH_3OH in D_2O , into a surrounding medium of 2 M CD_3OD in H_2O was therefore investigated. The experimental strategy was to acquire the volume-localized high resolution ^1H NMR spectrum from a volume element in the surrounding medium outside the membrane sac as a function of time, the voxel chosen being a cube of edge 4 mm. The distance from the top of the membrane sac to the bottom of the voxel was ca. 4.6 mm in each case. The volume localization protocol employed was ‘point resolved spectroscopy’ (PRESS) [30], the other relevant experimental parameters being: $\text{TR} = 2500$ ms, $\text{TE} = 13.408$ ms and $\text{NA} = 64$. Water suppression was carried out by the VAPOR sequence with 150 Hz bandwidth.

2.8. DMFC configuration and methanol permeation studies

The aforesaid membranes were used for their performance evaluation in DMFC by making membrane electrode assemblies (MEAs). Both the anode and cathode comprised a backing layer, a gas-diffusion layer (GDL) and a reaction layer. Teflonised Toray carbon papers (thickness = 0.37 mm) were employed as the backing layers in these electrodes. Diffusion layers comprising 1.5 mg/cm^2 of Vulcan XC-72R carbon slurry dispersed in isopropanol were applied onto the backing layers and sintered in a muffle furnace at 623 K for 30 min. 60 wt.% Pt/Ru (1:1 atomic ratio) supported on Vulcan XC-72R carbon mixed with binder and coated on to one of the GDL represented the catalyst layer on the anode, and 40 wt.% Pt catalyst supported on Vulcan XC-72R carbon mixed with binder coated on to the other GDL represented the catalyst layer on the cathode. The catalyst loading on both the anode and cathode was kept at 2 mg/cm^2 . The active area for the DMFC was 4 cm^2 . MEAs with PVA, PVA–PSSA blend and PVA–PSSA–MOR composite membranes were obtained by hot pressing at 15 kN (~ 60 kg/cm^2) at 353 K for 2 min.

MEAs were performance evaluated using a conventional fuel cell fixture with parallel serpentine flow field machined on graphite plates. The cells were tested at 343 K with 2 M aqueous methanol with a flow rate of 2 mL/min at the anode side and oxygen/air at the cathode side with a flow rate of 300 mL/min at atmospheric pressure. Measurements of cell potential as a function of current density were conducted galvanostatically using a Fuel Cell Test Station (Model PEM-FCTS-158541) supplied by Arbin Instruments (USA).

Methanol permeation studies from the anode to the cathode through the entire polymer electrolyte membranes in the DMFC were carried out as reported in the literature [31]. At the cathode,

the cross-over methanol from the anode was oxidized catalytically by a reaction with oxygen at the catalyst surface. The amount of cross-over methanol was analyzed gravimetrically by monitoring the CO_2 at the cathode exhausts. For this purpose, CO_2 from the cathode outlet was passed through a clear but saturated barium hydroxide $\text{Ba}(\text{OH})_2$ solution, which leads to the formation of barium carbonate (BaCO_3) precipitate according to the reaction:



BaCO_3 precipitate was separated from the liquid by a centrifuge, washed with DI water, and subsequently dried at 343 K for 24 h. After cooling to room temperature, it was weighed in a precision balance. The transport of methanol in a DMFC was visualized in terms of methanol permeation current. The methanol permeation current ($i_{\text{pmt}(\text{MeOH})}$ in mA) for the methanol cross-over from the anode to the cathode was obtained from Eq. (6) given below.

$$i_{\text{pmt}(\text{MeOH})} = \frac{6F(W_{\text{BaCO}_3})_c}{3600AM_{\text{BaCO}_3}} \quad (6)$$

The term on the right side of Eq. (6) refers to the equivalent current of total CO_2 flux collected at the cathode exhaust, F represents the Faraday constant, $(W_{\text{BaCO}_3})_c$ is the dry BaCO_3 weight collected at the cathode exhaust in 1 h (mg/h), A is the electrode area (cm^2) of the cell and M_{BaCO_3} is the molecular weight of BaCO_3 . The aforesaid procedure was repeated at different load current densities and the corresponding methanol permeation currents ($i_{\text{pmt}(\text{MeOH})}$ in mA) of the cross-over methanol were estimated. Based on the results of proton conductivity and methanol permeability, the electrochemical selectivity (β) of all the membranes was calculated using Eq. (7) given below [32].

$$\beta = \frac{\sigma}{P_{\text{MeOH}}} \quad (7)$$

where P_{MeOH} is the methanol permeability (cm^2/s) and σ is the proton conductivity (S/cm).

3. Results and discussion

3.1. Ion-exchange capacity (IEC) and degree of sulfonation (DS)

Ion-exchange capacity (IEC) provides an indicator of the ion-exchangeable groups present in a polymer matrix responsible for proton conduction. IEC value for Nafion-117 is 1.523 mequiv./g which is lower than the IEC values of 2.68 and 3.32 mequiv./g for PVA–PSSA (40% sulfonation) and PVA–PSSA (50% sulfonation), respectively. Average number of sulfonic groups present in the PSSA matrix represents the degree of sulfonation of PSSA and is around 40% and 50%, respectively, for two different PSSA matrices; 50% sulfonated PSSA appears to be a promising alternative proton exchange membrane since it has a higher IEC value.

3.2. Sorption

Liquid sorption through polymeric membranes has been well documented in the literature [33]. Sorption characteristics of Nafion-117, PVA, PVA–PSSA (40% sulfonation), PVA–PSSA (50% sulfonation) and PVA–PSSA–MOR composite membranes at 343 K in water are depicted in Figs. 1 and 2, respectively. It is noteworthy that sorption of all PVA–PSSA membranes increases with increasing degree of sulfonation and amount of mordenite from 3 to 10 wt.%. In Nafion-117 membrane, sorption is lower than other membranes due to the presence of hydrophobic fluorinated backbone and hydrophilic pendent chains that allow lower water uptake in relation to other membranes. By contrast, PVA and PVA–PSSA membranes exhibit higher water uptake due to their hydrophilic

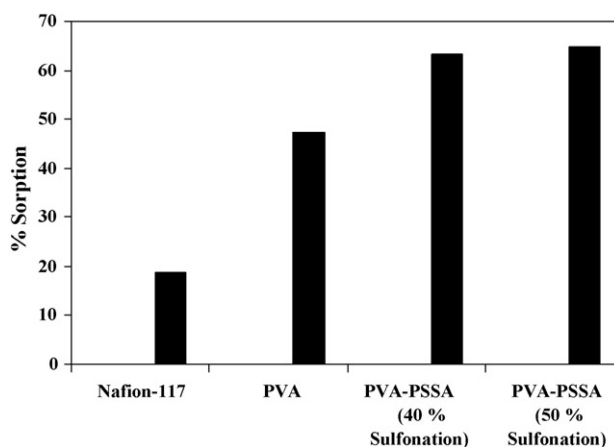


Fig. 1. Sorption (%) for Nafion-117, PVA, PVA–PSSA (40% sulfonation) and PVA–PSSA (50% sulfonation).

characteristic. Mordenite content in the PVA–PSSA membrane further enhances the hydrophilic nature with the maximum water uptake at about 10 wt.% mordenite in PVA–PSSA composite membrane. Hydrophilicity of PVA–PSSA–MOR membrane decreases for mordenite content > 10 wt.% possibly due to the blockage of polymer voids which reduce the degree of swelling as applicable for most of the fillers [34].

3.3. Proton conductivity

Proton transport occurs by the Grötthuss and the vehicular mechanisms where the protons jump from one solvent molecule to the other through hydrogen bonds, or diffuse together with solvent molecules [35]. Fig. 3 shows the proton conductivity of Nafion-117, pristine PVA, PVA–PSSA (40 and 50% sulfonation) blend and PVA–PSSA–MOR (3, 5, 10 and 15 wt.%) composite membranes as a function of temperature from 303 to 373 K. The proton conductivity for all the membranes increases with increasing temperature. It is realized that 50% sulfonated PVA–PSSA blend membrane exhibits higher proton conductivity due to its higher $-\text{SO}_3\text{H}$ content as compared to 40% sulfonated PVA–PSSA blend membrane. Both sorption and IEC have profound effect on membrane conductivity. Higher sorption promotes proton transport, and higher IEC decreases the distance between anionic groups leading to faster proton conduction. It is noteworthy that addition of mordenite to PVA–PSSA matrix increases its proton conductivity as protons take full advantage of proton-conducting mordenite pathways as well as

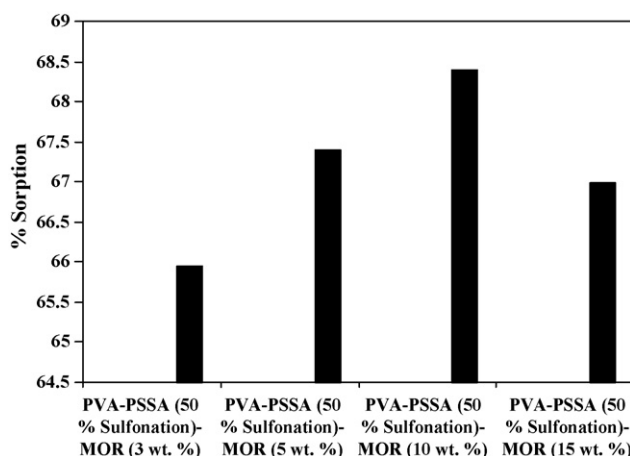


Fig. 2. Sorption (%) for PVA–PSSA (50% sulfonation)–mordenite (3, 5, 10 and 15 wt.%).

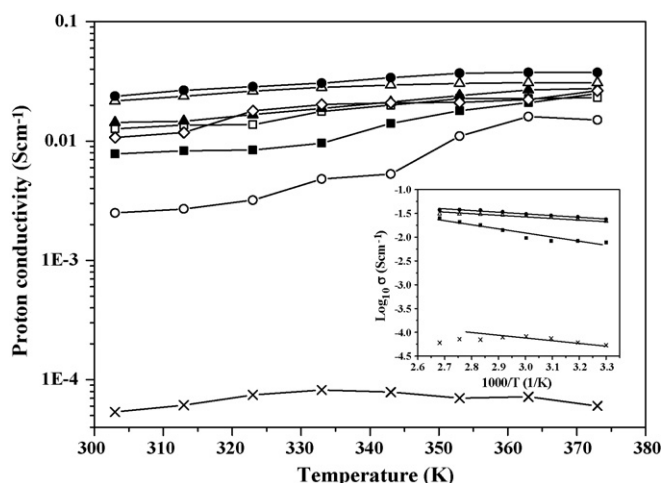


Fig. 3. Proton conductivity (σ) vs. temperature (T). Symbols: (\times) PVA; (\circ) PVA-PSSA (40% sulfonation); (\blacksquare) PVA-PSSA (50% sulfonation); (\square) PVA-PSSA-mordenite (3 wt.%) membrane; (\blacktriangle) PVA-PSSA-mordenite (5 wt.%) membrane; (\triangle) PVA-PSSA-mordenite (10 wt.%) membrane; (\diamond) PVA-PSSA-mordenite (15 wt.%) membrane; (\bullet) Nafion-117 membrane. Inset to the figure depicts the $\log_{10} \sigma$ vs. $1000/T$ plot. Symbols: (\times) PVA; (\blacksquare) PVA-PSSA (50% sulfonation); (\triangle) PVA-PSSA-mordenite (10 wt.%) membrane; (\bullet) Nafion-117 membrane.

voids in the polymer blend. However, higher content of mordenite (>10 wt.%) in PVA-PSSA blend disrupts the proton conduction path by blocking the voids of polymer matrix and decreases its proton conductivity.

All the membrane samples exhibit an Arrhenius-type temperature dependence of proton conductivity suggesting thermally activated proton conduction. The activation energy, which is the minimum energy required for proton transport, is obtained from the slope of Arrhenius plots using the relationship:

$$\sigma = \sigma_0 e^{-E_a/RT} \quad (8)$$

where σ is the proton conductivity in S/cm, σ_0 is the pre-exponential factor, E_a is the activation energy in kJ/mol, R is the universal gas constant (8.314 J/mol K), and T is the absolute temperature (K).

As proton conductivity (σ) is thermally activated, it is obvious to expect a rise in conductivity with temperature. The decay in conductivity values above 353 K observed for PVA membrane suggests dehydration of the membrane. Thus not only the capacity of the water uptake but also the capacity of the membrane to retain water at higher temperature is seminal for proton conductivity [27]. From the proton conductivity data presented in the inset to Fig. 3, the E_a value for proton conduction in PVA-PSSA (50% sulfonation) membrane is found to be 39.38 kJ/mol, which is higher than the E_a value of 4.32 kJ/mol for proton conduction in PVA membrane. This suggests that E_a for proton conduction increases with the introduction of PSSA in the PVA matrix. However, PVA-PSSA-MOR (10 wt.%) composite membrane exhibits lower activation energy (11.14 kJ/mol) for proton conduction than that for PVA-PSSA (50% sulfonation) membrane suggesting easy proton transport in the former membrane. Interestingly, Nafion membrane possesses E_a value of 15.22 kJ/mol for proton motion similar to that for PVA-PSSA-MOR (10 wt.%) composite membrane.

3.4. Mechanical stability

Mechanical stability of a membrane is seminal for its use in DMFCs. Tensile strengths and elongations at break for PVA, PVA-PSSA (40% sulfonation), PVA-PSSA (50% sulfonation) and PVA-PSSA-MOR (3, 5, 10 and 15%) composite membranes are compared with Nafion-117 membrane under dry condition in Table 1.

Table 1
Properties of Nafion, PVA, PVA-PSSA and PVA-PSSA-MOR membranes.

Membrane type	Tensile strength (N/mm ²)	Elongation at break (mm)	Average contact angle (°)	Surface wetting energy (mN/m)	t_1 (min) for water release kinetics (NMR imaging)	t_1 (min) for methanol release kinetics (volume localized NMR)	Electrochemical selectivity (S/cm ² s)
Nafion-117	78.53	7.2	75	19.11	—	—	0.81
PVA	28.37	2.3	—	—	—	—	0.65
PVA-PSSA (40% sulfonation)	37.98	3.7	—	—	—	—	1.45
PVA-PSSA (50% sulfonation)	43.22	3.9	60	36.44	41.69	365.59	1.60
PVA-PSSA (50% sulfonation)-MOR (3 wt.%)	52.56	4.5	—	—	—	—	2.36
PVA-PSSA (50% sulfonation)-MOR (5 wt.%)	61.15	5.6	—	—	—	—	2.99
PVA-PSSA (50% sulfonation)-MOR (10 wt.%)	72.89	6.9	37	57.77	50.78	1168.14	3.36
PVA-PSSA (50% sulfonation)-MOR (15 wt.%)	59.23	5.3	50	46.71	46.37	912.94	1.61

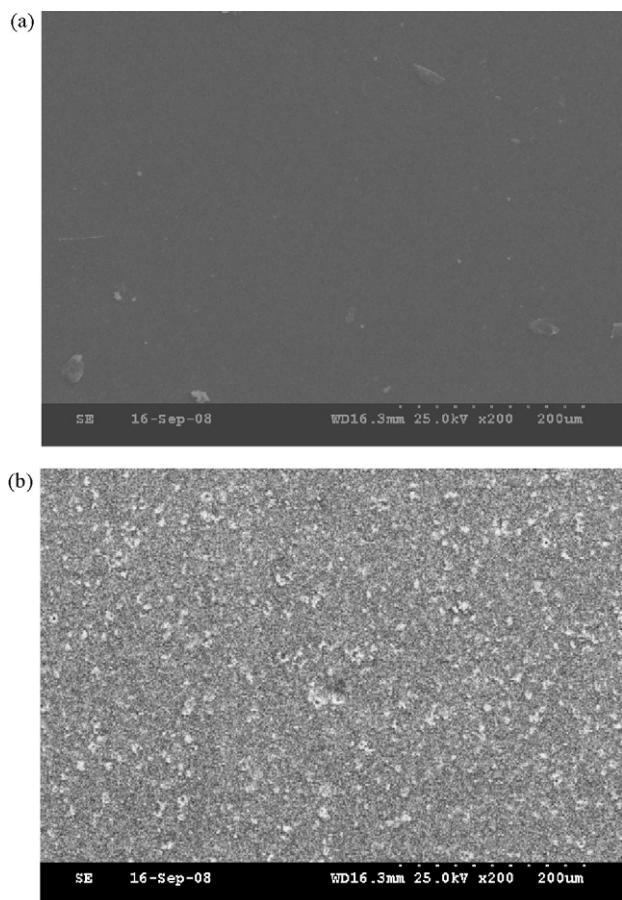


Fig. 4. (a) Surface SEM micrographs of PVA-PSSA (50% sulfonation) and (b) PVA-PSSA-mordenite (10 wt.%) membranes.

The data suggest that the tensile strength for the membranes increases with increasing mordenite content in the PVA-PSSA matrix from 3 to 10 wt.%. Introduction of MOR to the PVA-PSSA restricts the chain segmental mobility and increases the membrane strength. The membrane comprising 15 wt.% mordenite in the PVA-PSSA membrane shows a decrease in its mechanical properties due to its semi-brittle nature. By contrast, due to the flexible chain segmental mobility, the PVA-PSSA blend membrane exhibits low mechanical properties.

3.5. Membrane morphology

Fig. 4(a) and (b) elucidates the surface micrographs for PVA-PSSA (50% sulfonation) blend and PVA-PSSA-MOR (10 wt.%) composite membranes. A uniform distribution of MOR particles as a dispersed phase is clearly revealed in the PVA-PSSA matrix. It is noteworthy that MOR particles are beneficial for promoting water permeation while restricting methanol cross-over for its suitability in DMFCs.

3.6. Contact angle measurements

Since a liquid makes contact with the outermost molecular layer of a surface, contact angles are sensitive to chemical and physical changes that occur on the surface [36]. It is also known that the surfaces of the multiphase polymer blends are heterogeneous and comprise different types of domains [36]. In the present study, mordenite is a dispersed phase and PVA-PSSA is a continuous phase in which sessile water drop is added to find the contact angle at the solid-liquid interface. Table 1 shows the average contact

angles and surface wetting energies measured for different composite membranes. The average contact angle decreases sharply for 10 wt.% mordenite dispersion in PVA-PSSA and then increases for MOR dispersion >10 wt.% as dispersed phase reaches a critical coverage. It is noteworthy that contact angle for PVA-PSSA-MOR (10 wt.%) and PVA-PSSA membranes are lesser than that for Nafion-117 membrane since more hydrophilic chains are present in the former polymeric matrices which increase the surface wetting energy. However, for PVA-PSSA-MOR (15 wt.%) membrane, the average contact angle is increased and surface wetting energy is reduced due to the blockage of polymeric voids by higher addition of mordenite. These results suggest dual hydrophilic nature of the composite through dispersed phase of mordenite and continuous phase of PVA-PSSA matrix.

3.7. Thermogravimetric analysis

As shown in Fig. 5, TGA curves for Nafion-117, PVA, PVA-PSSA and PVA-PSSA-MOR membranes comprise three main degradation stages, namely thermal dehydration, thermal desulfonation, and thermal oxidation of the polymeric matrix [37,38]. The first weight loss of around 30 wt.% between 298 and 473 K is due to the removal of water from the PVA-PSSA blend and PVA-PSSA-MOR composite membranes while a weight loss of only about 10 wt.% is observed for pristine PVA and Nafion-117 membrane between 298 and 423 K. This suggests the water uptake for PVA-PSSA blend membranes to be higher than PVA and Nafion-117 membranes. Most of the water molecules in PVA-PSSA-MOR composite membranes are supposed to be bound directly to the polymer chains and/or the $-SO_3H$ groups through hydrogen bonds. The second weight loss of about 5 wt.% for Nafion-117 and 15 wt.% for PVA-PSSA blend and PVA-PSSA-MOR composite membranes are observed between 453 and 693 K, and correspond to loss of sulfonic acid groups by desulfonation. By contrast, no such weight loss is seen for pristine PVA membrane due to the absence of sulfonic acid groups. Sulfonic acid groups are bonded strongly in Nafion-117 than PVA-PSSA blend and PVA-PSSA-MOR composite membranes. This suggests that due to the high sulfonation level of PSSA, namely around 40% and 50%, the desulfonation weight loss is higher than that for Nafion-117 membrane. In the third weight loss regime, at temperatures >693 K, the polymer residues are further degraded due to the decomposition of main chains in PVA. By comparison, PVA membrane undergoes total thermal oxidation between 423 and 743 K due to the decomposition of its polymeric (side and main) chains. The remnant weight

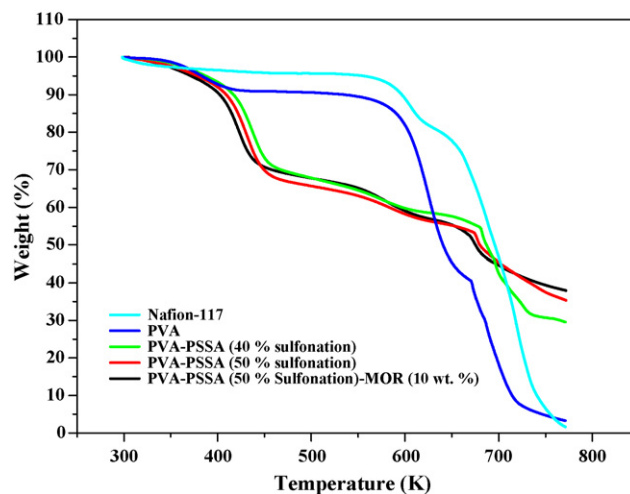


Fig. 5. TGA plots for Nafion-117, PVA, PVA-PSSA (40% sulfonation), PVA-PSSA (50% sulfonation) and PVA-PSSA-mordenite (10 wt.%) membranes.

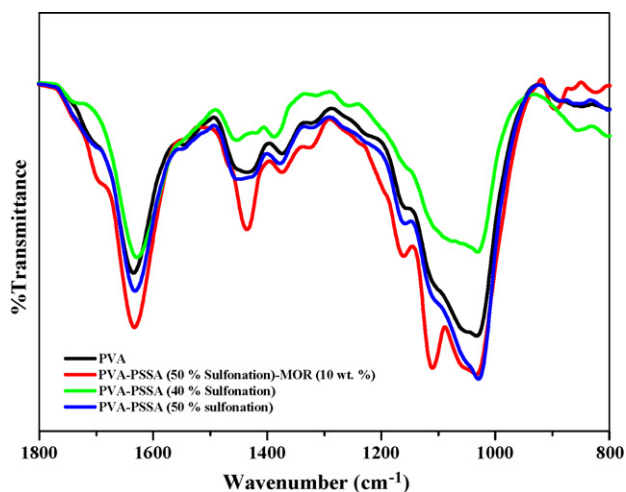


Fig. 6. FTIR plots for PVA, PVA-PSSA (40% sulfonation), PVA-PSSA (50% sulfonation) and PVA-PSSA-mordenite (10 wt.%) membranes.

after the polymer decomposition in all the membranes is due to the residual char. However, PVA-PSSA blend and PVA-PSSA-MOR composite membranes show lower weight loss in relation to PVA suggesting their higher thermal stability.

3.8. Fourier transform infrared spectroscopy (FTIR)

FTIR spectra for different composite membranes are shown in Fig. 6. For analysis of sulfonic groups and MOR present in PVA-PSSA-MOR matrix, FTIR spectra have been obtained over the range from 1800 to 800 cm^{-1} . The vibration band at 1040 cm^{-1} for PVA-PSSA (40% and 50% sulfonation) and PVA-PSSA-MOR membranes is attributed to the sulfonic group [39]. The peak identified in the spectra at 1400–1360 cm^{-1} is due to the asymmetric stretching of S=O bond for sulfonated membranes. The characteristic band at 1680 cm^{-1} (C=O) and C–O stretch mode at 1200 cm^{-1} , respectively, are due to the formation of C–O–C between alcohol group of PVA and carboxyl group of PSSA [40]. A sharp peak around 1101 cm^{-1} corresponds to Si–O bonds due to the presence of MOR and the peak at 900 cm^{-1} is attributed to Al–O stretching vibrations of MOR [41].

3.9. Spatially resolved NMR kinetic studies: diffusion of water from membrane sac to heavy water

Diffusion of water from membrane sacs of PVA-PSSA (50% sulfonated), PVA-PSSA (50% sulfonated + 10 wt.% mordenite) and PVA-PSSA (50% sulfonated + 15 wt.% mordenite) to surrounding D_2O [42] has been recorded at different time intervals by gradient echo imaging and some gradient echo images are presented in Fig. 7. The kinetics data culled from the image analysis are presented in Fig. 8 and summarized in Table 1. The equation used for fitting the curve is:

$$I(t) = I_0 + A_1 \exp\left(-\frac{t}{t_1}\right) \quad (9)$$

The mean intensity I of the water signal in a region of interest (ROI) chosen within the sac in the first image is plotted as a function of time. It may be noted that the kinetics of water release in these 'sac in D_2O ' experiments indicate that the PVA-PSSA (0% mordenite) membrane has the fastest release kinetics while the membrane with 10% mordenite shows the slowest release; the membrane with 15% mordenite being intermediate to these two limits. This validates the sorption data presented above.

3.10. Kinetic study: diffusion of CH_3OH from membrane sac to 2M CD_3OD in water

Diffusion of methanol from PVA-PSSA (50% sulfonated), PVA-PSSA (50% sulfonated + 10 wt.% mordenite) and PVA-PSSA

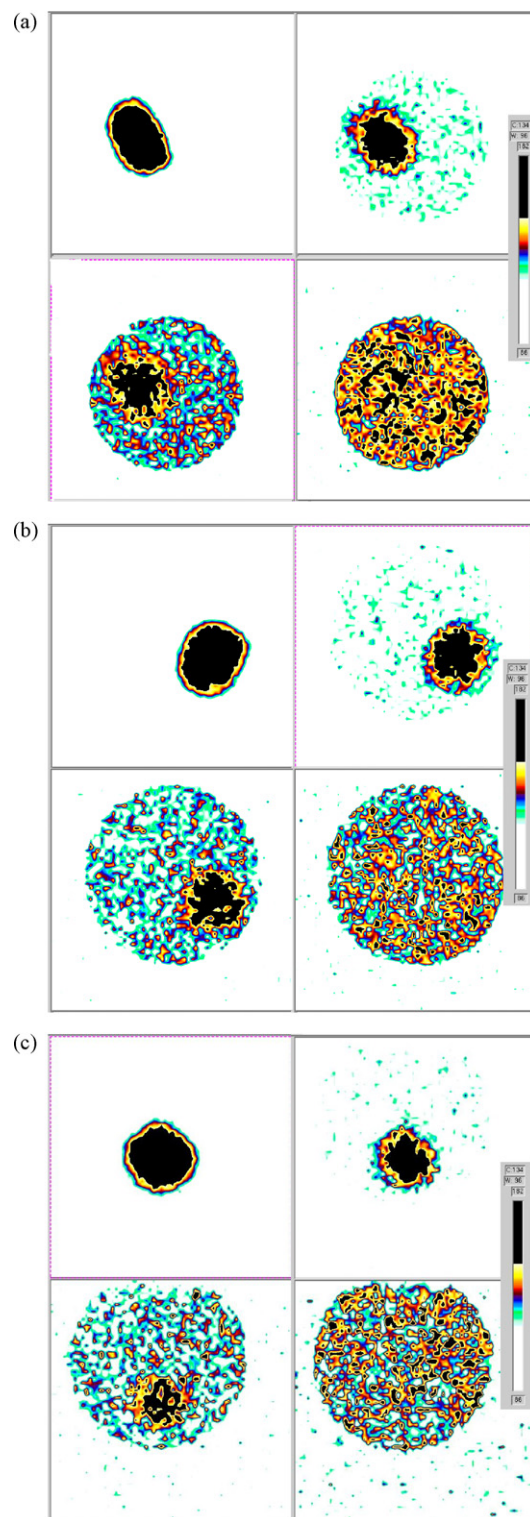


Fig. 7. (a) NMR images from left to right, top to bottom: 9, 59, 94 and 174 m after dropping PVA-PSSA sac in D_2O ; (b) NMR images from left to right, top to bottom: 13, 88, 118 and 233 m after dropping PVA-PSSA + 10 wt.% mordenite sac in D_2O ; (c) NMR images from left to right, top to bottom: 12, 72, 122 and 242 m after dropping PVA-PSSA + 15 wt.% mordenite sac in D_2O .

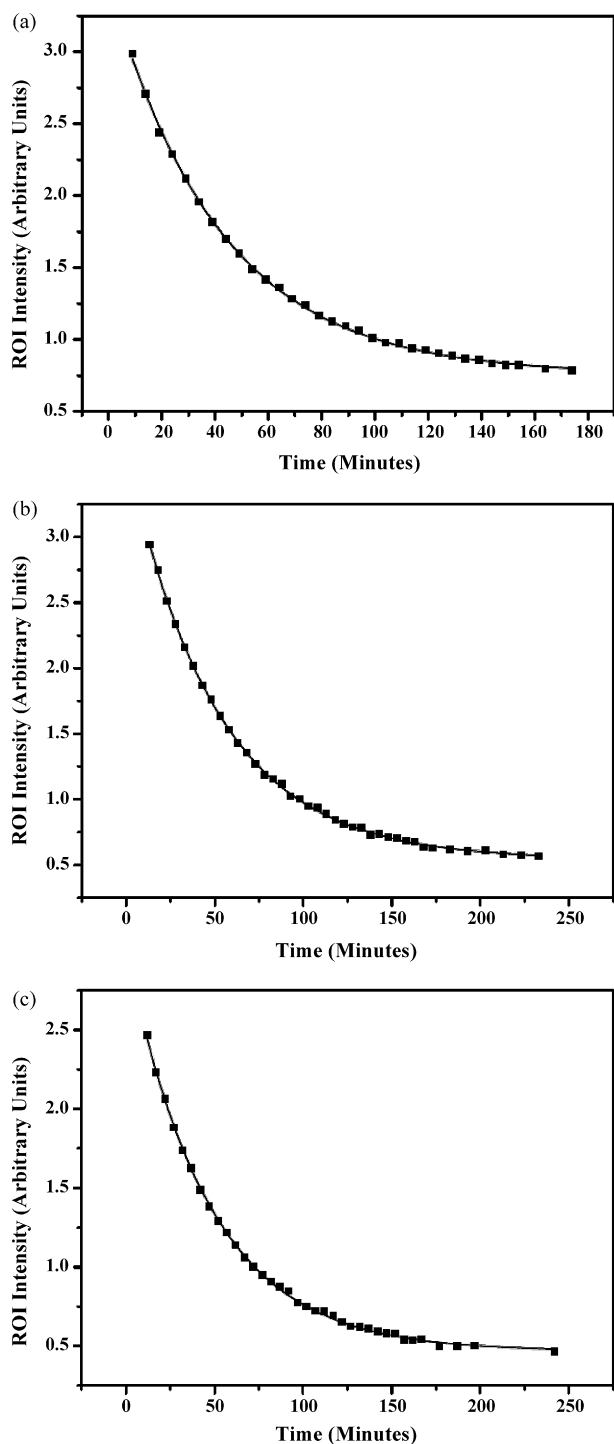


Fig. 8. Plot of water release kinetics of (a) PVA–PSSA sac, (b) PVA–PSSA + 10 wt.% mordenite sac, and (c) PVA–PSSA + 15 wt.% mordenite sac. All the plots were fitted with an exponential equation: $I(t) = I_0 - A_1 \exp(-t/t_1)$.

(50% sulfonated + 15 wt.% mordenite), each saturated with 2 M CH₃OH in D₂O to surrounding 2 M CD₃OD in water is recorded at different time intervals by PRESS spectroscopy [27]. It is noteworthy that the medium surrounding the membrane sac as employed in these studies, namely 2 M CD₃OD in water, permits the accurate determination of small differences in the release kinetics pertaining to different membranes by slowing down the overall release kinetics in comparison to a system that has only water surrounding the membrane sac. It may also be noted that ‘shimming’ the voxel of

interest is facilitated by water in the surrounding medium, although this signal is finally suppressed by standard outer volume suppression and specific water signal suppression procedures. The kinetics data are culled from the volume-localized spectral integral in the methyl region of the ¹H spectrum, the spectra being presented in Fig. 9(a)–(c), respectively. Eq. (10), given below, has been used for fitting the curve.

$$I(t) = I_0 - A_1 \exp\left(-\frac{t}{t_1}\right) \quad (10)$$

The mean integral I of the methyl signal in a voxel chosen to lie fully outside the sac has been plotted as a function of time in Fig. 10. It is noteworthy that the methanol release kinetics measurement clearly demonstrates that PVA–PSSA without mordenite has the highest methanol permeability while the membrane with 10% mordenite has the lowest; PVA–PSSA with 15% mordenite has an intermediate value (see Table 1).

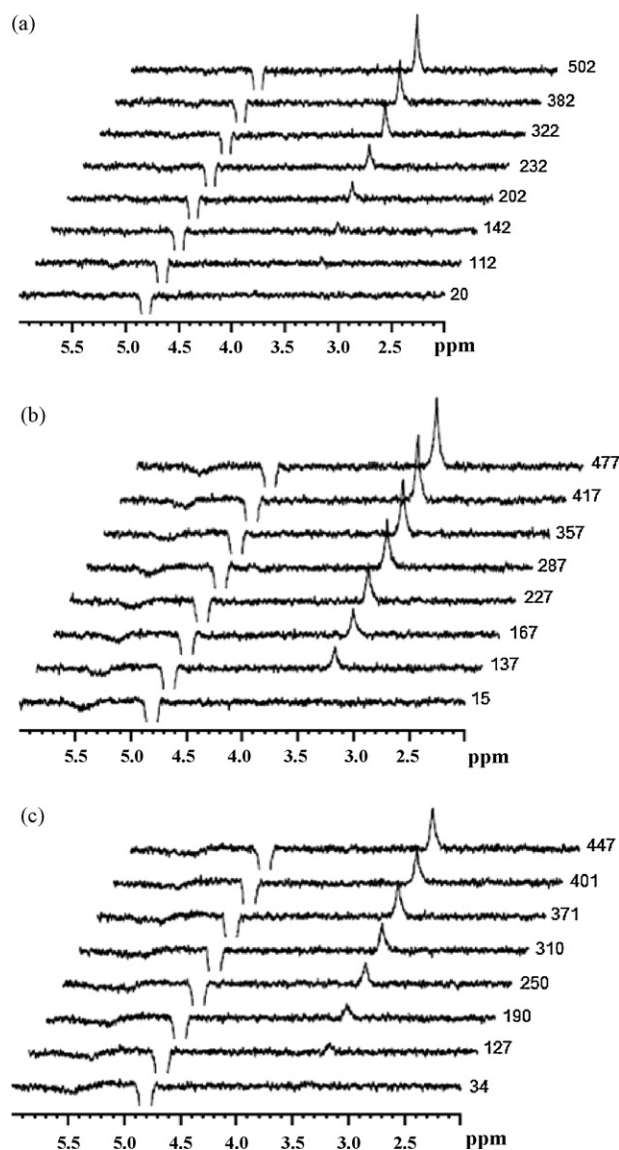


Fig. 9. Volume-localized spectra of methanol release from balls of (a) PVA–PSSA, (b) PVA–PSSA + 10 wt.% mordenite, and (c) PVA–PSSA + 15 wt.% mordenite, in each case after dropping the equilibrated sac in the solvent mixture. The time in minutes at which each measurement commenced after dropping the ball in the solvent mixture is indicated to the right of each spectral trace.

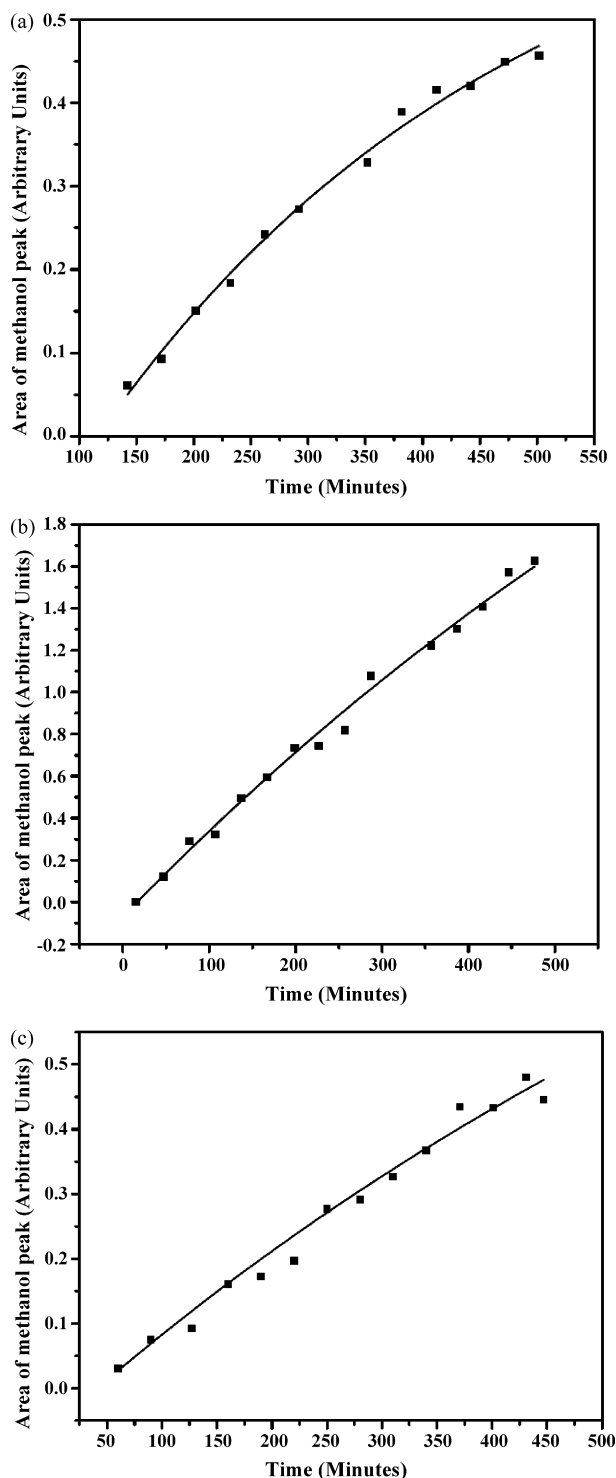


Fig. 10. Plots of the integral of the methyl signal of methanol vs. time for three different membrane sacs: (a) PVA–PSSA; (b) PVA–PSSA + 10 wt.% mordenite, and (c) PVA–PSSA + 15 wt.% mordenite. All the plots were fit with an exponential equation: $I(t) = I_0 - A_1 \exp(-t/t_1)$.

3.11. DMFC performance and methanol permeation study

Fig. 11(a) and (b) represents the DMFC performance curves for MEAs comprising Nafion-117, PVA, PVA–PSSA (40% sulfonation), PVA–PSSA (50% sulfonation) and PVA–PSSA–MOR (3, 5, 10 and 15 wt.%) composite membranes at 343 K. A peak power-density of 74 mW/cm² at a load-current density of 325 mA/cm² is observed for the DMFC with an MEA comprising PVA–PSSA (50%

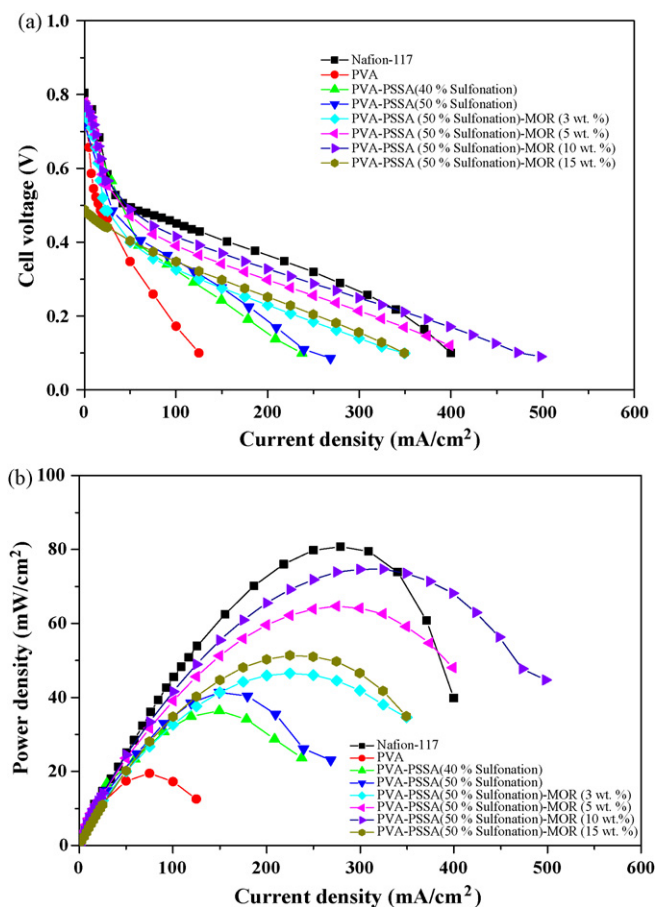


Fig. 11. (a) Cell voltage vs. current density and (b) power-density vs. current density for different types of membranes.

sulfonation)–MOR (10 wt.%) membrane which is slightly lower to the performance of MEA with Nafion-117 membrane. However, the peak power-density for pristine PVA membrane is found to be 19 mW/cm² at a load-current density of 74 mA/cm². This suggests higher proton conductivity for PVA–PSSA–MOR composite membrane than the PVA membrane. PVA–PSSA membranes with higher degree of sulfonation (i.e. 50%) show higher power-density than the membranes with lower degree of sulfonation (i.e. 40%) suggesting the influence of degree of sulfonation in the PSSA matrix. However, for MEAs with PVA–PSSA–MOR (3, 5 and 10 wt.%) membrane, the performance is further enhanced due to their higher proton conductivity and lower methanol cross-over than PVA–PSSA membranes. The maximum load-current density of 400 mA/cm² is achieved for MEA with Nafion-117 membrane as compared to the load-current density of 500 mA/cm² observed for PVA–PSSA–MOR which is due to the presence of dual hydrophilic chains in the latter. By contrast, a load-current density of 350 mA/cm² is observed for PVA–PSSA–MOR (15 wt.%) membrane suggesting the optimum content of mordenite to be 10 wt.%. The improved performance is due to the optimum tailoring of the polymer and dispersion phases in composite media where protons transport occurs directly through the polymer and zeolite phases while methanol faces a tortuous path around the zeolite particles [32].

Methanol permeation with respect to load-current density is shown in Fig. 12. Methanol permeation in Nafion-117 membrane is higher than PVA, PVA–PSSA and PVA–PSSA–MOR membranes but the performance for the DMFC using Nafion-117 membrane is superior owing to the higher proton conductivity of the latter in relation to other membranes. A methanol cross-over current as

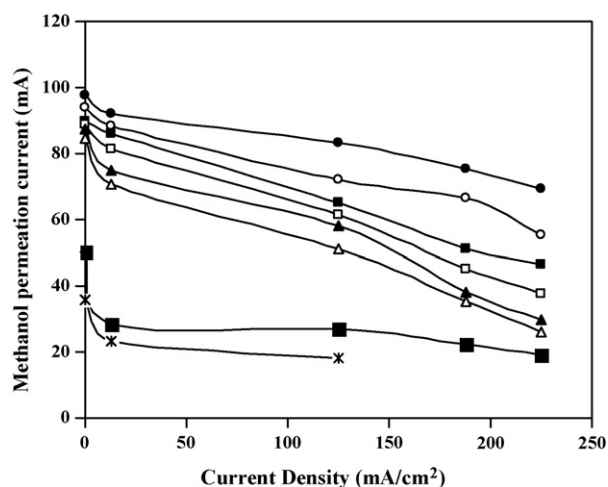


Fig. 12. Methanol permeability (mA) vs. current density (mA/cm^2). Symbols: (\times) PVA; (\circ) PVA-PSSA (40% sulfonation); (\blacksquare) PVA-PSSA (50% sulfonation); (\square) PVA-PSSA-mordenite (3 wt.%) membrane; (\blacktriangle) PVA-PSSA-mordenite (5 wt.%) membrane; (\triangle) PVA-PSSA-mordenite (10 wt.%) membrane; (\blacksquare) PVA-PSSA-mordenite (15 wt.%) membrane; (\bullet) Nafion-117 membrane.

low as $7.5 \text{ mA}/\text{cm}^2$ with 2 M methanol feed at the DMFC anode is observed while using the PVA-PSSA-MOR (10 wt.%) composite membrane as electrolyte in the DMFC, which is about 60% and 46%, lower than Nafion-117 and PVA-PSSA (50% sulfonation) membranes, respectively, tested under identical conditions. The hydrophilic nature of both PVA-PSSA and mordenite prevents the formation of non-selective voids for methanol transport at the polymer-zeolite interface without affecting the free transfer of protons as shown in Fig. 13.

Electrochemical selectivity allows a comparison of proton conductivity and methanol cross-over for different PVA-PSSA and PVA-PSSA-MOR membranes in relation to Nafion-117 membrane. A decrease in methanol permeability in PVA-PSSA and PVA-PSSA-MOR membranes accompanied with a smaller reduction in their proton conductivity in relation to Nafion-117 membrane demonstrates an improved electrochemical selectivity in the PVA-PSSA based membranes with increase in mordenite content. Table 1 shows the electrochemical selectivity for different membranes. PVA-PSSA-MOR (10 wt.%) membrane exhibits optimized balance between the methanol permeability and proton conductivity resulting in effective electrochemical selectivity with improved DMFC performance comparable to the DMFC with

Nafion-117 membrane. Lower methanol permeability and proton conductivity for PVA-PSSA-MOR (15 wt.%) membrane reduce its electrochemical selectivity in relation to PVA-PSSA-MOR (10 wt.%) membrane limiting the performance of the DMFC employing the former.

4. Conclusions

A new composite membrane comprising PVA-PSSA-MOR with reduced methanol permeability in relation to Nafion-117 membrane is reported. Spatially resolved NMR is found to be helpful in designing the PVA-PSSA membranes with varying contents of mordenite.

Acknowledgments

Financial support from CSIR, New Delhi as a Supra Institutional Project under EFYP is gratefully acknowledged. We thank Alwin, Nishanth and Jalajakshi for their valuable help. C.G. thanks UGC for a fellowship. N.C. thanks DST and IIT Madras for MRM and MRI system grants.

References

- [1] K. Scott, A.K. Shukla, in: R.E. White, C.G. Vayenas, M.A. Gamboa-Aldeco (Eds.), *Modern Aspects of Electrochemistry*, vol. 40, Springer, NY, 2006, pp. 127–218.
- [2] C.H. Rhee, H.K. Kim, H. Chang, J.S. Lee, Nafion/sulfonated montmorillonite composite: a new concept electrolyte membrane for direct methanol fuel cells, *Chem. Mater.* 17 (2005) 1691–1697.
- [3] M.K. Song, Y.M. Kim, Y.T. Kim, H.W. Rhee, A. Smirnova, N.M. Sammes, J.M. Fenton, Ultrathin reinforced nanocomposite membranes for direct methanol fuel cells, *J. Electrochem. Soc.* 153 (2006) A2239–A2244.
- [4] X. Ren, P. Zelenay, S. Thomas, J. Davey, S. Gottesfeld, Recent advances in direct methanol fuel cells at Los Alamos National Laboratory, *J. Power Sources* 86 (2000) 111–116.
- [5] K. Lee, J.D. Nam, Optimum ionic conductivity and diffusion coefficient of ion-exchange membranes at high methanol feed concentrations in a direct methanol fuel cell, *J. Power Sources* 157 (2006) 201–206.
- [6] K.D. Kreuer, On the development of proton conducting polymer membranes for hydrogen and methanol fuel cells, *J. Membr. Sci.* 185 (2001) 29–39.
- [7] H.L. Wu, C.C.M. Ma, C.H. Li, T.M. Lee, C.Y. Chen, C.L. Chiang, C. Wu, Sulfonated poly(ether ether ketone)/poly(amide imide) polymer blends for proton conducting membrane, *J. Membr. Sci.* 280 (2006) 501–508.
- [8] J. Won, S.W. Choi, Y.S. Kang, H.Y. Ha, I.H. Oh, H.S. Kim, K.T. Kim, H. Jo, Structural characterization and surface modification of sulfonated polystyrene-(ethylene-butylene)-styrene triblock proton exchange membranes, *J. Membr. Sci.* 214 (2003) 245–257.
- [9] H.B. Park, C.H. Lee, J.Y. Sohn, Y.M. Lee, B.D. Freeman, H.J. Kim, Effect of crosslinked chain length in sulfonated polyimide membranes on water sorption, proton conduction, and methanol permeation properties, *J. Membr. Sci.* 285 (2006) 432–443.
- [10] Y.J. Kim, W.C. Choi, S.I. Woo, W.H. Hong, Proton conductivity and methanol permeation in NafionTM/ORMOSIL prepared with various organic silanes, *J. Membr. Sci.* 238 (2004) 213–222.
- [11] W. Xu, T. Lu, C. Liu, W. Xing, Low methanol permeable composite Nafion/silica/PVA membranes for low temperature direct methanol fuel cells, *Electrochim. Acta* 50 (2005) 3280–3285.
- [12] C.H. Rhee, Y. Kim, J.S. Lee, H.K. Kim, H. Chang, Nanocomposite membranes of surface-sulfonated titanate and Nafion[®] for direct methanol fuel cells, *J. Power Sources* 159 (2006) 1015–1024.
- [13] C.W. Lin, K.C. Fan, R. Thangamuthu, Preparation and characterization of high selectivity organic-inorganic hybrid-laminated Nafion 115 membranes for DMFC, *J. Membr. Sci.* 278 (2006) 437–446.
- [14] M.A. Smit, A.L. Ocampo, M.A.E. Medina, P.J. Sebastian, A modified Nafion membrane with in situ polymerized polypyrrole for the direct methanol fuel cell, *J. Power Sources* 124 (2003) 59–64.
- [15] Z. Cui, N. Li, X. Zhou, C. Liu, J. Liao, S. Zhang, W. Xing, Surface-modified Nafion[®] membrane by casting proton-conducting polyelectrolyte complexes for direct methanol fuel cells, *J. Power Sources* 173 (2007) 162–165.
- [16] P. Dimitrova, K.A. Friedrich, U. Stimming, B. Vogt, Modified Nafion[®]-based membranes for use in direct methanol fuel cells, *Solid State Ionics* 150 (2002) 115–122.
- [17] Z. Cui, C. Liu, T. Lu, W. Xing, Polyelectrolyte complexes of chitosan and phosphotungstic acid as proton-conducting membranes for direct methanol fuel cells, *J. Power Sources* 167 (2007) 94–99.
- [18] B. Smitha, S. Sridhar, A.A. Khan, Polyelectrolyte complexes of chitosan and poly(acrylic acid) as proton exchange membranes for fuel cells, *Macromolecules* 37 (2004) 2233–2239.

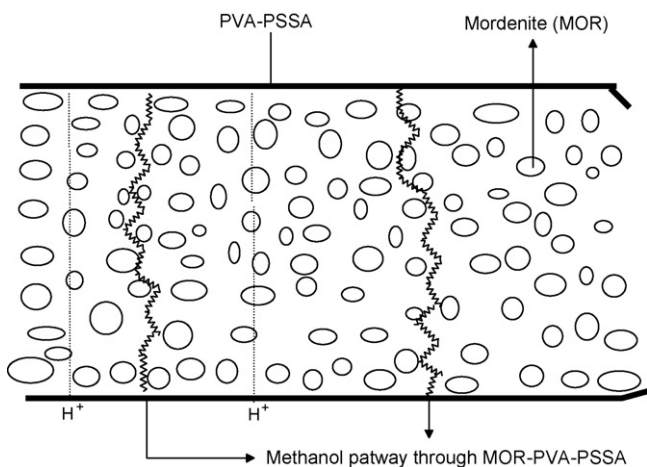


Fig. 13. Tortuous methanol and easy proton pathway through PVA-PSSA-mordenite composite membrane.

- [19] N. Carretta, V. Tricoli, F. Picchioni, Ionomeric membranes based on partially sulfonated poly(styrene): synthesis, proton conduction and methanol permeation, *J. Membr. Sci.* 166 (2000) 189–197.
- [20] H. Wu, Y. Wang, S. Wang, A methanol barrier polymer electrolyte membrane in direct methanol fuel cells, *J. New Mater. Electrochem. Syst.* 5 (2002) 251–254.
- [21] H. Jung, J.K. Park, Blend membranes based on sulfonated poly(ether ether ketone) and poly(vinylidene fluoride) for high performance direct methanol fuel cell, *Electrochim. Acta* 52 (2007) 7464–7468.
- [22] Z.G. Shao, I.M. Hsing, Nafion membrane coated with sulfonated poly(vinyl alcohol)–Nafion film for direct methanol fuel cells, *Electrochem. Solid-State Lett.* 5 (2002) A185–A187.
- [23] D. Kim, M.D. Guiver, S.Y. Nam, T. Yun, M.Y. Seo, S.J. Kim, H.S. Hwang, J.W. Rhim, Preparation of ion exchange membranes for fuel cell based on crosslinked poly(vinyl alcohol) with poly(styrene sulfonic acid-co-maleic acid), *J. Membr. Sci.* 281 (2006) 156–162.
- [24] C.W. Lin, Y.F. Huang, A.M. Kannan, Cross-linked poly(vinyl alcohol) and poly(styrene sulfonic acid-co-maleic anhydride)-based semi-interpenetrating network as proton-conducting membranes for direct methanol fuel cells, *J. Power Sources* 171 (2007) 340–347.
- [25] M.S. Kang, J.H. Kim, J. Won, S.H. Moon, Y.S. Kang, Highly charged proton exchange membranes prepared by using water soluble polymer blends for fuel cells, *J. Membr. Sci.* 247 (2005) 127–135.
- [26] B.S. Pivovar, Y. Wang, E.L. Cussler, Pervaporation membranes in direct methanol fuel cells, *J. Membr. Sci.* 154 (1999) 155–162.
- [27] A.K. Sahu, G. Selvarani, S. Pitchumani, P. Sridhar, A.K. Shukla, N. Narayanan, A. Banerjee, N. Chandrakumar, PVA–PSSA Membrane with interpenetrating networks and its methanol cross-over mitigating effect in DMFCs, *J. Electrochem. Soc.* 155 (2008) B686–B695.
- [28] D. Anjali Devi, B. Smitha, S. Sridhar, T.M. Aminabhavi, Dehydration of 1,4-dioxane through blend membranes of poly(vinyl alcohol) and chitosan by pervaporation, *J. Membr. Sci.* 280 (2006) 138–147.
- [29] B. Smitha, S. Sridhar, A.A. Khan, Synthesis and characterization of proton conducting polymer membranes for fuel cells, *J. Membr. Sci.* 225 (2003) 63–76.
- [30] P.A. Bottomley, Spatial localization in NMR spectroscopy *in vivo*, *Ann. N. Y. Acad. Sci.* 508 (1987) 333–348.
- [31] R. Jiang, D. Chu, Comparative studies of methanol cross-over and cell performance for a DMFC, *J. Electrochem. Soc.* 151 (2004) A69–A76.
- [32] B. Libby, W.H. Smyrl, E.L. Cussler, Polymer–zeolite composite membranes for direct methanol fuel cells, *AIChE J.* 49 (2003) 991–1001.
- [33] J. Crank, *The Mathematics of Diffusion*, Clarendon Press, Oxford, UK, 1975.
- [34] K. Prashantha, S.G. Park, Nanosized TiO₂-filled sulfonated polyethersulfone proton conducting membranes for direct methanol fuel cells, *J. Appl. Polym. Sci.* 98 (2005) 1875–1878.
- [35] K.D. Kreuer, On the complexity of proton conduction phenomena, *Solid State Ionics* 136–137 (2000) 149–160.
- [36] J.C. Lin, M. Ouyang, J.M. Fenton, H.R. Kunz, J.T. Koberstein, M.B. Cutlip, Study of blend membranes consisting of Nafion® and vinylidene fluoride-hexafluoropropylene copolymer, *J. Appl. Polym. Sci.* 70 (1998) 121–127.
- [37] A.K. Sahu, G. Selvarani, S.D. Bhat, S. Pitchumani, P. Sridhar, A.K. Shukla, N. Narayanan, A. Banerjee, N. Chandrakumar, Effect of varying poly(styrene sulfonic acid) content in poly(vinyl alcohol)–poly(styrene sulfonic acid) blend membrane and its ramification in hydrogen–oxygen polymer electrolyte fuel cells, *J. Membr. Sci.* 319 (2008) 298–305.
- [38] B.J. Holland, J.N. Hay, The thermal degradation of poly(vinyl alcohol), *Polymer* 42 (2001) 6775–6783.
- [39] F. Kucera, J. Jancar, Homogeneous and heterogeneous sulfonation of polymers: a review, *Polym. Eng. Sci.* 38 (1998) 783–792.
- [40] C.W. Lin, Y.F. Huang, A.M. Kannan, Semi-interpenetrating network based on cross-linked poly(vinyl alcohol) and poly(styrene sulfonic acid-co-maleic anhydride) as proton exchange fuel cell membranes, *J. Power Sources* 164 (2007) 449–456.
- [41] B.V.K. Naidu, S.D. Bhat, M. Sairam, A.C. Wali, D.P. Sawant, S.B. Halligudi, N.N. Mallikarjuna, T.M. Aminabhavi, Comparison of the pervaporation separation of a water–acetonitrile mixture with zeolite-filled sodium alginate and poly(vinyl alcohol)–polyaniline semi-interpenetrating polymer network membranes, *J. Appl. Polym. Sci.* 96 (2005) 1968–1978.
- [42] J. Kawamura, K. Hattori, T. Hongo, Y. Asayama, N. Kuwata, T. Hattori, J. Mizusaki, Microscopic states of water and methanol in Nafion membrane observed by NMR micro imaging, *Solid State Ionics* 176 (2005) 2451–2456.